NOTUM-MEDIATED WNT SILENCING DRIVES EXTRAVILLOUS TROPHOBLAST CELL LINEAGE DEVELOPMENT

Vinay Shukla[1,*], Ayelen Moreno-Irusta[1], Kaela M. Varberg[1,†], Marija Kuna[1], Khursheed Iqbal[1,‡], Anna M. Galligos[1,¶], John D. Aplin[2,3], Ruhul H. Choudhury[2,3], Hiroaki Okae[4], Takahiro Arima[5], and Michael J. Soares[1,6,7,*]

[1]Institute for Reproductive and Developmental Sciences, Department of Pathology and Laboratory Medicine, University of Kansas Medical Center, Kansas City, KS

[2]Maternal and Fetal Health Research Centre, Division of Developmental Biology and Medicine, The University of Manchester, Manchester M13 9WL, United Kingdom

[3]Manchester Academic Health Sciences Centre, St Mary's Hospital, University of Manchester, Manchester M13 9WL, United Kingdom

[4]Department of Trophoblast Research, Institute of Molecular Embryology and Genetics, Kumamoto University, Kumamoto 860-0811 Japan

[5]Department of Informative Genetics, Environment and Genome Research Center, Tohoku University Graduate School of Medicine, Sendai 980-8575, Japan

[6]Center for Perinatal Research, Children's Research Institute, Children's Mercy, Kansas City, MO

[7]Department of Obstetrics and Gynecology, University of Kansas Medical Center, Kansas City, KS

[*]Correspondence should be addressed: vshukla@kumc.edu or msoares@kumc.edu

[†]Present address: Department of Pediatrics, Children's Mercy Research Institute, Children's Mercy, Kansas City, MO

[‡]Present address: Department of Animal and Food Sciences, Oklahoma State University, Stillwater, OK

[¶]Present address: Stowers Institute for Medical Research, Kansas City, MO

Running title: NOTUM and trophoblast cell differentiation

***Key Words*: Placenta, NOTUM, WNT, extravillous trophoblast cells**

ABSTRACT

Trophoblast stem (**TS**) cells have the unique capacity to differentiate into specialized cell types, including extravillous trophoblast (**EVT**) cells. EVT cells invade into and transform the uterus where they act to remodel the vasculature facilitating the redirection of maternal nutrients to the developing fetus. Disruptions in EVT cell development and function are at the core of pregnancy-related disease. WNT-activated signal transduction is a conserved regulator of morphogenesis of many organ systems, including the placenta. In human TS cells, activation of canonical WNT signaling is critical for maintenance of the TS cell stem state and its downregulation accompanies EVT cell differentiation. We show that aberrant WNT signaling undermines EVT cell differentiation. Notum, palmitoleoyl-protein carboxylesterase (**NOTUM**), a negative regulator of canonical WNT signaling, was prominently expressed in first trimester EVT cells developing in situ and upregulated in EVT cells derived from human TS cells. Furthermore, NOTUM was required for human TS cell differentiation to EVT cells. Activation of NOTUM in EVT cells is driven, at least in part, by endothelial PAS domain 1 (also called hypoxia-inducible factor 2 alpha). Collectively, our findings indicate that canonical WNT signaling is essential for maintenance of human trophoblast cell stemness and prevention of human TS cell differentiation. Downregulation of canonical WNT signaling via the actions of NOTUM is required for EVT cell differentiation.

SIGNIFICANCE

Extravillous trophoblast (**EVT**) cells play a critical role in transforming the uterine environment into a supportive organ facilitating embryonic/fetal development. Insufficient EVT cell-dependent uterine transformation can lead to obstetrical complications, including early pregnancy loss, preeclampsia, intrauterine growth restriction, and preterm birth. These complications carry a significant burden of morbidity and mortality for both the mother and the fetus. Notum, palmitoleoyl-protein carboxylesterase, a WNT signaling antagonist, is involved in promoting and maintaining EVT cell differentiation. This process is essential for the proper development of the placenta and is crucial for a healthy pregnancy.

INTRODUCTION

Development of the human placenta is necessary for proper embryonic development and successful pregnancy outcome (**1**). The hemochorial placenta develops through tightly regulated expansion and differentiation of trophoblast stem (**TS**) cells (**2**). Human TS cells can differentiate into two specialized cell types: syncytiotrophoblast and extravillous trophoblast (**EVT**) cells (**3-5**). Syncytiotrophoblast regulates maternal and fetal homeostasis through hormone production and control of the transfer of nutrients between maternal and fetal compartments, whereas EVT cells facilitate transformation of the uterus into a structure supportive of fetal growth and development (**4, 5**). EVT cells restructure uterine vasculature to optimize nutrient flow to the placenta (**6-8**). Abnormalities in EVT cell invasion and uterine spiral artery remodeling have been detected in an assortment of pregnancy disorders such as early pregnancy loss, preeclampsia, intrauterine growth restriction, and preterm birth (**9, 10**). Thus, experimental investigation of mechanisms underlying the derivation of the invasive EVT cell lineage could represent a key to understanding the etiology of placental dysfunction leading to pregnancy related disorders. At this juncture, there is a paucity of knowledge regarding the regulation of TS cells and especially their differentiation into EVT cells.

WNT signaling has been implicated as a key regulator of morphogenesis of many developing organ systems (**11**). WNT proteins represent a family of ligands that act by interacting with members of the Frizzled (**FZD**) receptor protein family (**11, 12**). Effective recognition by FZD proteins requires the post-translational addition of a palmitoleate moiety to WNT (**13, 14**), which is performed by Porcupine O-acyltransferase (**15**). Palmitoylated WNT is a target of Notum, Palmitoleoyl-protein Carboxylesterase (**NOTUM**), a secreted deacylase (**16, 17**). NOTUM removes the palmitoleate moiety from WNT, which destabilizes WNT interactions with FZD and negates downstream WNT/FZD-mediated signal transduction (**16, 17**). Canonical WNT signaling involves the redistribution of β-catenin (**CTNNB1**) from the cell membrane to the nucleus where it interacts with members of the lymphoid enhancer binding factor-1 (**LEF1**)/T cell factor (**TCF**) family of transcription factors (**12, 18**).

WNT signaling has been implicated in the regulation of placental development (**19-21**). WNT ligands are expressed within the early embryo (**22, 23**) and throughout the placentation site (**24**). A broad spectrum of activities has been ascribed to canonical WNT signaling in placental

morphogenesis. These include roles in maintaining trophoblast cells in the stem/proliferative state (**25, 26**) and in promoting differentiation into syncytiotrophoblast (**27, 28**) and EVT cells (**29-31)**. Supporting both the stem state and cell differentiation would seem to be opposing efforts but may reflect actions that are developmental stage and context dependent. Disruptions in canonical WNT signaling have also been connected to diseases of placentation (**32, 33**)

In this report, we evaluate the role of canonical WNT signaling in the regulation of human TS cell differentiation to EVT cells. The capture and ex vivo propagation of human TS cells represented a breakthrough for investigating human trophoblast cell differentiation (**25**). These cells can be maintained in a stem state or induced to differentiate into syncytiotrophoblast or EVT cells. We demonstrate that canonical WNT signaling blocks EVT cell differentiation and discover a critical role for NOTUM in facilitating EVT cell differentiation through silencing canonical WNT signaling.

RESULTS

WNT activation disrupts EVT cell differentiation

Canonical WNT signaling supports maintenance of human TS cells in the stem state (**25**). Initially, using the human TS cell model (**Fig. 1A**), we monitored canonical WNT signaling by assessing active CTNNB1 (dephosphorylated on Ser-37 and Thr-41) using immunofluorescence in human TS cells maintained in the stem state and following EVT cell differentiation. Active CTNNB1 was abundant in stem cell nuclei but not in EVT cell nuclei, suggesting that WNT signaling was downregulated during EVT cell development (**Fig. 1B**) and supporting the involvement of WNT signaling in maintenance of the stem state. Standard culture conditions used to promote the TS cell stem state include the glycogen synthase kinase 3 (**GSK3**) inhibitor, CHIR99021, an activator of canonical WNT signaling (**25**). In contrast, culture conditions promoting EVT cell differentiation exclude CHIR99021 (**25**). We next sought to directly determine the consequences of activation of WNT signaling (CHIR99021) on EVT cell differentiation.

CHIR99021 was added as a supplement to the standard EVT cell differentiation culture conditions of X,X CT27 human TS cells (**25**). We examined the effects of WNT activation throughout EVT cell differentiation. Microscopy and immunofluorescence analyses revealed that addition of CHIR99021 resulted in the accumulation of active CTNNB1 in the nucleus (**Fig. 1C**) and an inhibition of EVT cell differentiation. The elongated/spindle-shaped cells characteristic of in vitro EVT cell differentiation were not observed following induction of WNT signaling (**Fig. 1D**). EVT cell signature transcripts (e.g. *HLA-G*, *MMP2*, and *ASCL2*) and major histocompatibility complex, class I, G (**HLA-G**) protein were decreased in TS cells exposed to EVT cell differentiating conditions supplemented with CHIR99021 (**Fig. 1E, F**). We extended this analysis to an investigation of the effects of WNT activation on the EVT cell transcriptome (**Fig. 1G, H and Dataset 1**). RNA sequencing (**RNA-seq**) identified 3,663 differentially expressed genes (**DEGs**), including 1,536 transcripts upregulated and 2,127 transcripts downregulated by exposure to CHIR99021. Stem state signature transcripts (e.g. *LRP2*, *TEAD4*, *MKI67*) were upregulated and EVT cell signature transcripts (e.g. *HLA-G*, *MMP2*, *ASCL2*, *FSTL3*, *NOTUM*) were downregulated (**Fig. 1H**). This differential gene expression pattern was validated by reverse transcriptase-quantitative PCR (**RT-qPCR**) (***SI Appendix,* Fig. S1**). In addition, trophoblast cell invasiveness was examined using Matrigel® Transwell assays. WNT activation inhibited EVT cell

migration (**Fig. 1I and J**). We next examined the short-term effects of CHIR99021 withdrawal during the TS cell stem state and prolonged WNT activation until late in the EVT cell differentiation process. Evidence for EVT cell differentiation was observed within 48 h of CHIR99021 withdrawal as demonstrated by significant enhancement of the expression of some EVT signature transcripts (***SI Appendix,* Fig. S2**). Prolonged WNT activation did not significantly affect the expression of EVT cell signature transcripts, except for *AOC1* (***SI Appendix,* Fig. S3**), a measure of late-stage EVT cell maturation (**34**).

Overall, these results demonstrated that canonical WNT signaling had a prominent restraining role on the initiation of EVT cell differentiation with potentially some modest effects promoting late stage EVT cell maturation. We next sought evidence to determine whether canonical WNT signaling was operational in the first trimester human placenta.

Canonical WNT signaling in the human placentation site

To assess the role of WNT signaling in the developing human placenta, we examined the distribution of active CTNNB1 and major histocompatibility complex, class I, G (**HLA-G**) protein in first trimester placental tissue specimens. Activated CTNNB1 was prominently expressed in cytotrophoblast populations, including the basal cytotrophoblast and cells within the transition zone of the EVT cell column (**Fig. 2A**). Co-expression of active CTNNB1 and HLA-G was not observed (**Fig. 2B and C**). We extended this analysis to the decidual bed and observed co-localization of CTNNB1 and HLA-G in intrauterine endovascular EVT cells (**Fig. 2D-F**). Thus, in situ development of the EVT cell lineage within the EVT cell column does not appear compatible with expression of activated CTNNB1; however, canonical WNT signaling may contribute to the development and/or function of later stage intrauterine endovascular EVT cells.

We were next directed to elucidating endogenous mechanisms during EVT differentiation responsible for liberating TS cells from the restraining actions of WNT signaling.

NOTUM is expressed in EVT cells

Inspection of RNA-seq datasets from human TS cells in stem and EVT cell differentiated states (**25, 35**) showed that *NOTUM* was prominently activated during EVT cell differentiation. The EVT cell-dependent upregulation of NOTUM was verified by RT-qPCR, western blotting, and

immunofluorescence (**Fig. 3A-C**). These observations prompted an investigation of *NOTUM* expression in the first trimester human placenta. *NOTUM*, *CDH1,* and *PLAC8* transcripts were assessed by in situ hybridization. *CDH1* is a marker of a proliferative population of cytotrophoblast situated at the base of EVT cell columns (**35, 36**), whereas *PLAC8* is distinctively expressed in EVT cells situated in the distal part of EVT cell columns (**35, 37**). Within the EVT cell column *NOTUM* did not co-localize with *CDH1* (**Fig. 3D**) but instead co-localized with *PLAC8* (**Fig. 3E**). This analysis was extended to first trimester placental bed specimens where mature EVT cells invade deep into the uterine decidua (**38**). *NOTUM* was co-localized with *KRT8*, a marker of EVT cells (**Fig. 3F**). These findings are consistent with the detection of NOTUM expression in second trimester EVT cells (**39**). Thus, NOTUM is expressed in EVT cells differentiated from TS cells in vitro and within invading EVT cells identified in situ within first and second trimester human placentation sites.

NOTUM promotes EVT cell differentiation

We hypothesized that NOTUM removes WNT-mediated inhibition of EVT cell differentiation. To test our hypothesis, we used a *loss-of-function* approach to determine whether NOTUM is required for EVT cell differentiation. NOTUM expression was silenced in X,X CT27 human TS cells using stable lentiviral-mediated delivery of short hairpin RNAs (**shRNA**) targeted to NOTUM. Disruption of NOTUM expression was verified by RT-qPCR and western blotting (**Fig. 4A, B**). TS cells expressing NOTUM shRNAs failed to show appropriate morphologic indices of EVT cell differentiation (**Fig. 4C**) and did not exhibit the characteristic upregulation of signature EVT cell transcripts (e.g., *HLA-G, MMP2, ASCL2, FSTL3, TFPI*) (**Fig. 4D**), or HLA-G protein expression (**Fig. 4E**). We extended this analysis to an investigation of the effects of NOTUM silencing on the EVT cell transcriptome (**Fig. 4F, G and Dataset 2**). RNA-seq analysis identified 1,340 DEGs, including 543 upregulated transcripts and 797 downregulated transcripts in NOTUM knockdown cells. Consistent with morphologic observations and candidate transcript assessments, we identified a significant upregulation of stem state-specific transcripts (e.g., *LRP2*, *TEAD4*, *YAP1*, *F3*) and downregulation of EVT cell-specific transcripts (e.g., *HLA-G*, *MMP2*, *TFPI*, *ASCL2*, *CDKN1C*, *PLOD2*) (**Fig. 4G, Dataset 2, *SI Appendix,* Fig. S4**). Disruption of NOTUM also inhibited acquisition of the invasive properties of EVT cells (**Fig. 4H, I**) and resulted in activation of canonical WNT signaling as demonstrated by the presence of nuclear active CTNNB1 (***SI Appendix,* Fig. S5**). Similar to roles

for canonical WNT activation and NOTUM silencing on X,X CT27 EVT cell differentiation, these experimental manipulations negatively impacted X,Y CT29 EVT cell differentiation (***SI Appendix,* Fig. S6**). We also examined the consequences of nullifying the actions of NOTUM using a small molecule inhibitor, LP922056 (**40**). This similarly interfered with EVT cell differentiation (***SI Appendix,* Fig. S7**). Thus, NOTUM promotes EVT cell differentiation.

Upstream regulation of NOTUM

We next sought to investigate the control of NOTUM expression in differentiating EVT cells. Inspection of RNA-seq profiles from earlier efforts of our laboratory indicated that endothelial PAS domain protein 1 (**EPAS1**) was a potential upstream regulator of NOTUM (**35**). EPAS1 protein has been referred to as hypoxia-inducible factor 2 alpha (**HIF2A**). NOTUM and EPAS1 exhibited parallel patterns of expression in TS cells in the stem state and following their differentiation into EVT cells (**Fig. 5A, B**). Inhibition of EPAS1 expression in human TS cells resulted in the downregulation of NOTUM transcript and protein expression (**Fig. 5 C, D**). These observations support a role for EPAS1/HIF2A as an upstream regulator of *NOTUM*. Glial cell missing 1 (**GCM1**) has also been identified as a potential upstream regulator of *NOTUM* (**41, 42**) and EPAS1 as a potential upstream regulator of *GCM1* in differentiating EVT cells (**35**).

Collectively, the findings indicate that NOTUM is required for acquisition of structural, molecular, and functional indices of EVT cell differentiation and are consistent with its restraining actions on canonical WNT signaling.

DISCUSSION

Our findings indicate that suppression of canonical WNT signaling is critical for human TS cell differentiation into EVT cells. In vitro EVT cell differentiation is accompanied by extensive cell elongation and spreading and the upregulation of transcripts indicative of the EVT cell fate (e.g., *HLA-G*, *MMP2*) (**25**). Consistent with these observations, we found that addition of a potent WNT activator, CHIR99021 (GSK3B inhibitor), inhibited differentiation of TS cells into EVT cells. We next interrogated human TS cells in stem and EVT differentiation states for expression of components of the WNT

signaling pathway with the goal of identifying potential endogenous regulators of WNT signaling. Among the upregulated transcripts, NOTUM expression was striking in terms of both magnitude of the increase and overall expression level. NOTUM antagonizes WNT signaling by facilitating the depalmitoloylation of WNT proteins, which impairs their binding to frizzled receptors (**40**). Importantly, the differentiation-associated increase in NOTUM expression was required for optimal EVT cell differentiation. Upstream activation of NOTUM was regulated, at least in part, by the transcription factor, EPAS1. Collectively, our findings indicate that WNT drives trophoblast cell stemness, while EVT cell differentiation is facilitated by WNT suppression through the actions of NOTUM.

Findings presented herein indicate that WNT possesses a critical and primary role in maintaining trophoblast cell stemness and antagonizes differentiation. This observation differs from other research showing roles for WNT signaling in promoting EVT cell differentiation (**29-31**). These WNT actions on the TS cell stem state versus EVT cell differentiation are proposed to be managed through different members of the TCF family, which are downstream effectors WNT signaling (**26**). We observed that extended WNT activation in human TS cells could influence some parameters characteristic of EVT cells. Furthermore, intrauterine endovascular EVT cells expressed activated CTNNB1. The observed differences in the spectrum of WNT actions on trophoblast cells are likely consequences of the range of in vitro model systems and measures used to assess EVT cell behavior.

Despite the recognized significance of WNT signaling in trophoblast cell biology (**43-45**), a role for NOTUM in this process was not previously recognized. WNT signaling is a conserved regulator of placentation in the human and mouse (**43-45**). In contrast, NOTUM appears to be a species-specific regulator of the invasive trophoblast cell lineage, which may be best exemplified in comparing rat with human placentation. The rat exhibits robust intrauterine trophoblast cell invasion (**46, 47**) but invasive trophoblast cells do not express detectable NOTUM, instead rat invasive trophoblast cells express other WNT signaling antagonists, including catenin beta interacting protein 1 (**CTNNBIP1**) and NKD inhibitor of WNT signaling pathway 1 (**NKD1**) (**48**). It remains to be determined whether and how WNT signaling and WNT antagonists may modulate development and function of the rat invasive trophoblast cell lineage.

Overall, canonical WNT signaling is pivotal to the maintenance of human TS cell stemness and prevention of EVT cell differentiation. NOTUM is identified as a critical liberator of canonical WNT dominance leading to development of EVT cells. Thus, the appropriate modulation of canonical WNT signaling is critical to placental development and its dysregulation a potential factor in placental disease.

MATERIALS AND METHODS

Human placentation site specimens

Sections from paraffin-embedded deidentified first trimester human placenta and placental bed tissue specimens were obtained from the Lunenfeld-Tanenbaum Research Institute (Mount Sinai Hospital, Toronto, Canada) and St. Mary's Hospital, Manchester, United Kingdom, respectively. Tissue collections were performed after written informed consent. Institutional approval was obtained from Human Research Ethics Review Committees at the University of Toronto, Central Manchester Health Trust, and the University of Kansas Medical Center (**KUMC**).

TS cell culture

Cytotrophoblast-derived CT27 (X,X) and CT29 (X,Y) lines were used in the experiments. Human TS cells were maintained in stem state conditions or induced to differentiate into syncytiotrophoblast or EVT cells as previously described (**25**). Human TS cells were cultured in six-well plates precoated with 5 μg/mL of Corning™ collagen IV (CB40233, Thermo Fisher) and Basal Human TS Cell Medium [Dulbecco's Modified Eagle Medium/F12 (DMEM/F12, 11320033, Thermo Fisher) containing 100 μM 2-mercaptoethanol, 0.2% (vol/vol), fetal bovine serum (**FBS**), 50 μM penicillin, 50 U/mL streptomycin, 0.3% bovine serum albumin (BP9704100, Thermo Fisher), 1% Insulin-Transferrin-Selenium-Ethanolamine solution (**ITS-X**, vol/vol, Thermo Fisher), supplemented with 1.5 μg/mL L-ascorbic acid (A8960, Sigma-Aldrich), 50 ng/mL epidermal growth factor (**EGF**, E9644, Sigma-Aldrich), 2 μM CHIR99021 (04-0004, Reprocell), 0.5 μM A83-01 (04-0014, Reprocell), 1 μM SB431542 (04-0010, Reprocell), 0.8 mM valproic acid (P4543, Sigma-Aldrich), and 5 μM Y27632 (04-0012-02, Reprocell).

EVT cell differentiation was performed as previously described (**25**). Human TS cells were plated onto a 6-well plate precoated with 1 μg/mL collagen IV at a density of 1×10^5 cells per well and

cultured in EVT Cell Differentiation Medium, which consists of Basal Human TS Cell Medium supplemented with 100 ng/mL of neuregulin 1 (**NRG1**, 5218SC, Cell Signaling), 7.5 μM A83-01, 2.5 μM Y27632, 4% KnockOut Serum Replacement (**KSR**, 10828028, Thermo Fisher), and 2% Matrigel (CB-40234, Fisher). On day 3 of EVT cell differentiation, the medium was replaced with the EVT Cell Differentiation Medium without NRG1, and the Matrigel® concentration was decreased to 0.5%. On day 6 of EVT cell differentiation, the medium was replaced with EVT Cell Differentiation Medium without NRG1 or KSR and with Matrigel® at a concentration of 0.5%. Cells were analyzed on day 8 of EVT cell differentiation or in one set of experiments, the culture was extended to day 14 of EVT cell differentiation.

TS cells were induced to differentiate into syncytiotrophoblast using three-dimensional (3D) culture conditions [**ST(3D)**] (**25**). TS cells (2.5 x 10^5) were seeded into six cm Petri dishes and cultured in 3 mL of ST(3D) medium containing DMEM/F12 supplemented with 100 μM 2-mercaptoethanol, 0.5% penicillin-streptomycin, 0.3% BSA, 1% ITS-X supplement, 2.5 μM Y27632, 50 ng/ml EGF, 2 μM forskolin (F6886, Sigma-Aldrich), and 4% KSR. An equal amount of fresh ST(3D) media was added at day 3. Cells were passed through a 40 μm mesh filter to remove dead cells and debris at day 6. Cells remaining on the 40 μm mesh filter were collected and analyzed.

shRNAs, transient transfection, lentivirus production and transduction

A lentiviral-mediated shRNA delivery approach was used to silence *NOTUM* and *EPAS1* gene expression. *NOTUM* shRNAs were designed and subcloned into the pLKO.1 vector at *AgeI* and *EcoRI* restriction sites. *EPAS1* shRNAs were described previously (**35**). shRNA sequences used in the analyses are included in **Table S1**. Lentiviral packaging vectors were obtained from Addgene and included pMDLg/pRRE (plasmid 12251), pRSVRev (plasmid 12253), and pMD2.G (plasmid 12259). Lentiviral particles were produced following transient transfection of the shRNA-pLKO.1 vector and packaging plasmids into Lenti-X cells (632180; Takara Bio USA) using Attractene (301005; Qiagen) in Opti-MEM I (51985-034; Thermo Fisher). Thereafter, cells were maintained in DMEM (11995-065; Thermo Fisher) with 10% FBS. Culture supernatants containing lentiviral particles were collected every 24 h for two days and stored frozen at -80°C until use.

Human TS cells were plated at 80,000 cells per well in 6-well tissue culture-treated plates coated with 5 μg/mL collagen IV (CB40233; Thermo Fisher) and incubated for 24 h. Just before transduction, medium was changed, and cells were incubated with 2.5 μg/mL polybrene for 30 min at 37°C. Immediately following polybrene incubation, TS cells were transduced with 500 μL of lentiviral particle supernatant and then incubated for 24 h. Medium was changed at 24 h post-transduction and selected with puromycin dihydrochloride (5 μg/mL, A11138-03; Thermo Fisher) for 2 days. Cells were allowed to recover for 1 to 3 days in complete human TS medium before splitting for EVT cell differentiation.

Matrigel invasion assay

Invasiveness was assessed by plating cells on Matrigel-coated transwell inserts with 8.0 μm transparent polyester membrane pores (Corning, 353097), as previously described (**49**). Briefly, EVT cells were dissociated into single cells and seeded at a density of 2×10^5 cells per well into the upper chamber of Matrigel-coated transwells in 200 μL EVT Cell Differentiation Medium. The lower chamber was filled with 750 μL of the EVT Cell Differentiation Medium containing 20% FBS. EVTs were cultured at 37°C in 5% CO_2. After 36 h, a cotton swab moistened with medium was inserted into the top of the Matrigel matrix-coated permeable support (apical side) and gentle but firm pressure was used to remove cells from the support. The lower chamber was fixed with 4% paraformaldehyde, washed with phosphate buffered saline (pH 7.4), and next stained with crystal violet. Invaded cells were imaged on a Nikon Eclipse 80i microscope. Subsequently, stained cells from three random fields were counted to calculate the relative fold change in the number of invading cells.

Immunofluorescence

Human TS cells or differentiated EVT cells were fixed with 4% paraformaldehyde (Sigma-Aldrich) for 20 min at room temperature. Immunofluorescence analysis was performed using a primary antibody against NOTUM (1:500, SAB3500082, Sigma-Aldrich), active-CTNNB1 (1:400, clone 8E7, 05-665, Sigma-Aldrich), HLA-G (1:400, ab52455; Abcam), or EPAS1/HIF2A (1:500, D6T8V, rabbit monoclonal antibody 59973, Cell Signaling). Alexa Fluor 488 goat anti-mouse IgG (1:800, A32723 Thermo Fisher), Alexa Fluor 568 goat anti-mouse IgG (1:800, A11031, Thermo Fisher), Alexa Fluor 568 goat anti-rabbit IgG, (1:800, A10042, Thermo Fisher) were used to detect locations of the

primary antibody-antigen complexes within cells and tissues. For immunohistochemical analysis, paraffin-embedded slides incubated with 10% normal goat serum (50062Z; Thermo Fisher Scientific) for 1 h. Sections were incubated overnight with primary antibodies: NOTUM (1:500, SAB3500082, Sigma-Aldrich), active-CTNNB1 (1:400, clone 8E7, 05-665, Sigma-Aldrich), HLA-G (1:400, ab52455; Abcam), or EPAS1/HIF2A (1:500, D6T8V, rabbit monoclonal antibody 59973, Cell Signaling). After washing with phosphate-buffered saline (pH 7.4), sections were incubated for 2 h with corresponding secondary antibodies: Alexa Fluor 488 goat anti-mouse IgG (1:800, A32723 Thermo Fisher), Alexa Fluor 568 goat anti-mouse IgG (1:800, A11031, Thermo Fisher), Alexa Fluor 568 goat anti-rabbit IgG, (1:800, A10042, Thermo Fisher). Nuclei were visualized by staining with 4'6'-diamidino-2-phenylindole (**DAPI**, Molecular Probes). Immunostained sections were mounted in Fluoromount-G (0100-01; SouthernBiotech). Images were captured on a Nikon 80i upright microscope with a Roper Photometrics CoolSNAP-ES monochrome camera.

Western blot analysis

Cell lysates were prepared by sonication in radioimmunoprecipitation assay lysis buffer (sc-24948A, Santa Cruz Biotechnology) supplemented with Halt protease and phosphatase inhibitor mixture (78443, Thermo Fisher). Protein concentrations were measured using the DC Protein Assay (5000113-115, Bio-Rad). Proteins (20 µg/lane) were separated by sodium dodecyl sulfate polyacrylamide gel electrophoresis and transferred onto polyvinylidene difluoride membranes (10600023, GE Healthcare). After transfer, membranes were blocked with 5% non-fat milk/BSA in Tris buffered saline with 0.1% Tween 20 (**TBST**) and probed with primary antibodies to NOTUM (1:1500, SAB3500082, Sigma-Aldrich), HLA-G (1:1000. ab52455, Abcam), total CTNNB1 (1:1000, clone D10A8, 8480, Cell Signaling), active-CTNNB1 (1:1000, clone 8E7, 05-665, Sigma-Aldrich), phosphorylated CTNNB1 (1:1000, Ser33/37/Thr41, 9561 Cell Signaling), EPAS1 (1:300, 66731-1-Ig, Proteintech) and glyceraldehyde-3-phosphate dehydrogenase (ab9485; Abcam) overnight at 4°C. Membranes were washed three times for five min each with TBST and then incubated with secondary antibodies (goat anti-rabbit IgG HRP, A0545, Sigma Aldrich; goat anti-mouse IgG HRP, 7076; Cell Signaling) for 1 h at room temperature. Immunoreactive proteins were visualized by enhanced chemiluminescence according to the manufacturer's instructions (Amersham).

In situ hybridization

Detection of NOTUM transcripts was performed on paraffin-embedded human placentation site tissue sections using the RNAscope Multiplex Fluorescent Reagent Kit version 2 (Advanced Cell Diagnostics), according to the manufacturer's instructions. RNAscope probes were used to detect *NOTUM* (NM_178493.5, 430311, target region: 259-814), *PLAC8* (NM_016619.3, 858491-C2, target region: 5-1448), *KRT8* (NM_002273.4, 310261-C2, target region: 279-1171), and *CDH1* (NM_004360.3, 311091-C2, target region: 263-1255). Fluorescence images were captured on a Nikon 80i upright microscope (Nikon) with a Roper Photometrics CoolSNAP-ES monochrome camera (Roper).

RNA isolation, cDNA synthesis, and RT-qPCR

Total RNA was isolated from cells with TRIzol reagent (15596018, Thermo Fisher) as described previously (**50**). cDNA was synthesized from 1 µg of total RNA using a High-Capacity cDNA Reverse Transcription Kit (4368813; Thermo Fisher) and diluted 10 times with Milli-Q water. Reverse transcriptase-polymerase chain reaction (**RT-qPCR**) was performed using a reaction mixture containing PowerSYBR Green PCR Master Mix (4367659, Thermo Fisher) and primers (250 nM each). PCR primer sequences are presented in **Table S2**. Real-time PCR amplification and fluorescence detection were carried out using a QuantStudio 7 Flex Real-Time PCR System (Thermo Fisher). An initial step (95 °C, 10 min) preceded 40 cycles of a two-step PCR at the following conditions: 92 °C, for 15 s and 60 °C for 1 min, followed by a dissociation step (95 °C for 15 s, 60 °C for 15 s, and 95 °C for 15 s). The comparative cycle threshold method was used for relative quantification of the amount of mRNA for each sample normalized to a housekeeping gene *GAPDH*.

RNA-seq analysis

RNA-seq was performed as previously described (**51**). Transcript profiles were generated from vehicle control and CHIR99021 (2 μM) or control shRNA and NOTUM shRNA exposures in CT27 human TS cells cultured in conditions promoting EVT cell differentiation (n=3 experiments per group, each sample corresponded to a distinct transduction). Complementary DNA libraries from total RNA samples were prepared with Illumina TruSeq RNA preparation kits according to the manufacturer's instructions. RNA integrity was assessed using an Agilent 2100 Bioanalyzer. Barcoded cDNA libraries

were multiplexed onto a TruSeq paired-end flow cell and sequenced (100-bp paired-end reads) with a TruSeq 200-cycle SBS kit (Illumina). Samples were run on Illumina HiSeq2500 sequencers located at the KUMC Genome Sequencing Facility. Reads from *.fastq files were mapped to the human reference genome (GRCh37) using CLC Genomics Workbench 12.0 (Qiagen). Transcript abundance was expressed as reads per kilobase of transcript per million mapped reads (**RPKM**), DEGs were identified using false discovery rate (**FDR**) and fold change (**FC**) versus control groups (FDR<0.05; FC≥1.5). Statistical significance was calculated by empirical analysis of digital gene expression followed by Bonferroni's correction. QIAGEN Ingenuity Pathway Analysis of DEGs was performed to gain additional insight into the biological impacts of the cell/molecular manipulations.

Statistical analysis

Statistical analyses were performed with GraphPad Prism 9 software. Student's *t* test, one-way or two-way analysis of variance were applied as appropriate. Statistical significance was determined as P<0.05. All values are presented as the mean ± standard error of the mean (**SEM**) of at least three independent experiments.

Data availability

The datasets generated and analyzed for this study have been deposited in the Gene Expression Omnibus (GEO) database, https:// www.ncbi.nlm.nih.gov/geo/ (accession no. GSE206036).

ACKNOWLEDGMENTS

The research was supported by postdoctoral fellowships by the KUMC Biomedical Research Training Program and K-INBRE (P20 GM103418; VS, AM, MK), a Lalor Foundation Fellowship (AM), and an NIH National Research Service Award postdoctoral fellowship (HD096809, KMV) and NIH grants (HD020676, HD079363, HD099638, HD105734), and the Sosland Foundation. We thank Stacy Oxley and Brandi Miller for administrative assistance.

Competing interests

No competing interests.

REFERENCES

1. G.J. Burton, A.L. Fowden, K.L. Thornburg, Placental origins of chronic disease. *Physiol. Rev.* **96**, 1509-1565 (2016).

2. M. Hemberger, C.W. Hanna, W. Dean, Mechanisms of early placental development in mouse and humans. *Nat. Rev. Genet.* **21**, 27-43 (2020).

3. E. Maltepe, S.J. Fisher, Placenta: the forgotten organ. *Annu. Rev. Cell Dev. Biol.* **31**, 523-552 (2015).

4. M. Knöfler, *et al*., Human placenta and trophoblast development: key molecular mechanisms and model systems. *Cell Mol. Life Sci.* **76**, 3479-3496 (2019).

5. M.J. Soares, K.M. Varberg, K. Iqbal, Hemochorial placentation: development, function, and adaptations. *Biol. Reprod.* **99**, 196-211 (2018).

6. R. Pijnenborg, L. Vercruysse, M. Hanssens, The uterine spiral arteries in human pregnancy: facts and controversies. *Placenta* **27**, 939-958 (2006).

7. L.K. Harris, Trophoblast-vascular cell interactions in early pregnancy: how to remodel a vessel. *Placenta* **31**(Suppl), S93-S98 (2010).

8. P. Velicky, M. Knöfler, J. Pollheimer, Function and control of human invasive trophoblast subtypes: Intrinsic vs. maternal control. *Cell Adh. Migr.* **10**, 154-162 (2016).

9. S.J. Fisher, Why is placentation abnormal in preeclampsia? Am. J. Obstet. Gynecol. 213, S115-S122 (2015).

10. I. Brosens, P. Puttemans, G. Benagiano, Placental bed research: I. The placental bed: from spiral arteries remodeling to the great obstetrical syndromes. *Am. J. Obstet. Gynecol.* **221**, 437-456 (2019).

11. A. Wodarz, R. Nusse, Mechanisms of Wnt signaling in development. *Annu. Rev. Cell Dev. Biol.***14**, 59-88 (1998).

12. E.Y. Rim, H. Clevers, R. Nusse, The Wnt pathway: from signaling mechanisms to synthetic modulators. *Annu. Rev. Biochem.* **91**, 571-598 (2022).

13. K. Willert, *et al.*, Wnt proteins are lipid-modified and can act as stem cell growth factors. *Nature* **423**, 448-452 (2003).

14. C.Y. Janda, D. Waghray, A.M. Levin, C. Thomas, K.C. Garcia, Structural basis of Wnt recognition by Frizzled. *Science* **337**, 59-64 (2012).

15. R. Takada R, *et al*., Monounsaturated fatty acid modification of Wnt protein: its role in Wnt secretion. *Dev. Cell* **11**, 791-801 (2006).

16. S. Kakugawa, *et al.*, Notum deacylates Wnt proteins to suppress signalling activity. *Nature* **519**, 187–192 (2015).

17. X. Zhang, *et al.,* Notum is required for neural and head induction via Wnt deacylation, oxidation, and inactivation. *Dev. Cell* **32**, 719–730 (2015).

18. S. Söderholm, C. Cantù, The WNT/β-catenin dependent transcription: A tissue-specific business. WIREs Mech. Dis. 13, e1511 (2021).

19. S. Sonderegger, J. Pollheimer, M. Knöfler, Wnt signalling in implantation, decidualisation and placental differentiation--review. *Placenta* **31**, 839-847 (2010).

20. M. Knöfler, J. Pollheimer, Human placental trophoblast invasion and differentiation: a particular focus on Wnt signaling. *Front. Genet.* **4**, 190 (2013).

21. B. Dietrich, S. Haider, G. Meinhardt, J. Pollheimer, M. Knöfler, WNT and NOTCH signaling in human trophoblast development and differentiation. *Cell Mol. Life Sci.* **79**, 292 (2022).

22. H. Xie, et al., Inactivation of nuclear Wnt-beta-catenin signaling limits blastocyst competency for implantation. *Development* **135**, 717-727 (2008).

23. M. Krivega, W. Essahib, H. Van de Velde, WNT3 and membrane-associated β-catenin regulate trophectoderm lineage differentiation in human blastocysts. *Mol. Hum. Reprod.* **21**, 711-722 (2015).

24. S. Sonderegger, H. Husslein, C. Leisser, M. Knöfler, Complex expression pattern of Wnt ligands and frizzled receptors in human placenta and its trophoblast subtypes. *Placenta* **28**, S97-S102 (2007).

25. H. Okae *et al.,* Derivation of human trophoblast stem cells. *Cell Stem Cell* **22**, 50-63.e6 (2018).

26. S. Haider, *et al.,* Self-renewing trophoblast organoids recapitulate the developmental program of the early human placenta. *Stem Cell Reports* **11**, 537–551 (2018).

27. K. Matsuura, *et al*., Identification of a link between Wnt/β-catenin signalling and the cell fusion pathway. *Nat. Commun*. **2**, 548 (2011).

28. D. Zhu, X. Gong, L. Miao, J. Fang, J. Zhang, Efficient induction of syncytiotrophoblast layer II cells from trophoblast stem cells by canonical Wnt signaling activation. *Stem Cell Reports* **9**, 2034-2049 (2017).

29. J. Pollheimer, *et al.,* Activation of the canonical wingless/T-cell factor signaling pathway promotes invasive differentiation of human trophoblast. *Am. J. Pathol.* **168**, 1134-1147 (2006).

30. S. Sonderegger, *et al.,* Wingless (Wnt)-3A induces trophoblast migration and matrix metalloproteinase-2 secretion through canonical Wnt signaling and protein kinase B/AKT activation. *Endocrinology* **151**, 211-220 (2010).

31. G. Meinhardt, *et al*., Wnt-dependent T-cell factor-4 controls human extravillous trophoblast motility. *Endocrinology* **155**, 1908-1920 (2014).

32. X. Wang, *et al*., Wnt/β-catenin signaling pathway in severe preeclampsia. *J. Mol. Histol.* **49**, 317-327 (2018).

33. Y. Liu, J. Huang, N. Yu, S. Wei, Z. Liu, Involvement of WNT2 in trophoblast cell behavior in preeclampsia development. *Cell Cycle* **9**, 2207-2215 (2020).

34. P. Velicky, *et al*., Pregnancy-associated diamine oxidase originates from extravillous trophoblasts and is decreased in early-onset preeclampsia. *Sci. Rep.* **8**, 6342 (2018).

35. K.M. Varberg, *et al*., Extravillous trophoblast cell lineage development is associated with active remodeling of the chromatin landscape. *Nat. Commun.* **14**, 4826 (2023).

36. S.J. Renaud, *et al*., OVO-like 1 regulates progenitor cell fate in human trophoblast development. *Proc. Natl. Acad. Sci. USA* **112**, E6175-E6184 (2015).

37. W.L. Chang, *et al*., PLAC8, a new marker for human interstitial extravillous trophoblast cells, promotes their invasion and migration. *Development* **145**, dev148932 (2018).

38. R.H. Choudhury, *et al.,* Extravillous trophoblast and endothelial cell crosstalk mediates leukocyte infiltration to the early remodeling decidual spiral arteriole wall. *J. Immunol.* **198**, 4115-4128 (2017).

39. J.F. Robinson *et al.,* Transcriptional dynamics of cultured human villous cytotrophoblasts. *Endocrinology* **158**, 1581-1594 (2017).

40. E.D. Bayle, *et* al., Carboxylesterase Notum is a druggable target to modulate Wnt signaling. *J. Med. Chem.* **64**, 4289-4311 (2021).

41. M.J. Jeyarajah, *et al*., The multifaceted role of GCM1 during trophoblast differentiation in the human placenta. *Proc. Nat.l Acad. Sci. USA* **119**, e2203071119 (2022).

42. T. Shimizu, et al., CRISPR screening in human trophoblast stem cells reveals both shared and distinct aspects of human and mouse placental development. *Proc. Natl. Acad. Sci. USA*, in press (2023).

43. S. Sonderegger, J. Pollheimer, M. Knofler, Wnt signalling in implantation, decidualization and placental differentiation. *Placenta* **31**, 839-847 (2010).

44. M. Knofler, J. Pollheimer, Human placental trophoblast invasion and differentiation: a particular focus on Wnt signaling. *Front. Genet.* **4**, 190 (2013).

45. B. Dietrich, S. Haider, G. Meinhardt, J. Pollheimer, M. Knofler, WNT and NOTCH signaling in human trophoblast development and differentiation. *Cell Mol. Life Sci.* **79**, 292 (2022).

46. R. Ain, L.N. Canham, M.J. Soares, Gestation stage-dependent intrauterine trophoblast cell invasion in the rat and mouse: novel endocrine phenotype and regulation. *Dev. Biol.* **260**, 176-90 (2003).

47. V. Shukla, M.J. Soares, Modeling Trophoblast cell-guided uterine spiral artery transformation in the rat. Int. J. Mol. Sci. 23:2947 (2022).

48. R.L. Scott et al., Conservation at the uterine-placental interface. *Proc. Natl. Acad. Sci. USA* **119**, e2210633119 (2022).

49. M. Kuna et al., CITED2 is a conserved regulator of the uterine-placental interface. *Proc. Natl. Acad. Sci. USA* **120**, e2213622120 (2023).

50. K.M. Varberg *et al.,* ASCL2 reciprocally controls key trophoblast lineage decisions during hemochorial placenta development. *Proc. Natl. Acad. Sci. USA* **118**, e2016517118 (2021).

51. M. Muto *et al.,* Intersection of regulatory pathways controlling hemostasis and hmochorial placentation. *Proc. Nat.l Acad. Sci. USA* **118**, e2111267118 (2021).

FIGURES

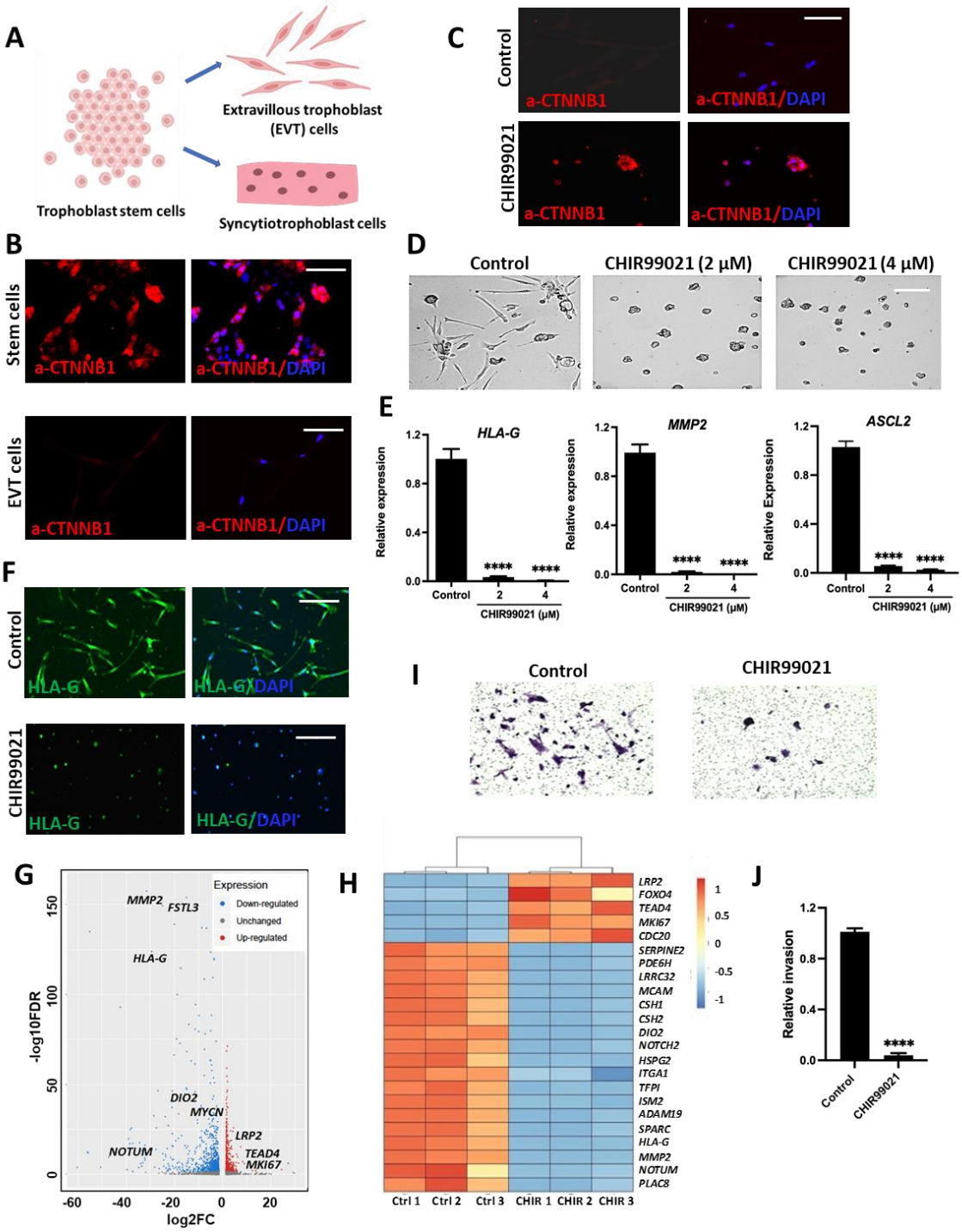

Fig. 1. WNT activation disrupts extravillous trophoblast (**EVT**) cell differentiation. *(A)* Schematic depicting trophoblast cell differentiation from the stem state toward either EVT cell or syncytiotrophoblast fates. *(B)* Immunocytochemistry of active CTNNB1 (a-CTNNB1) protein expression (red) in stem and EVT cells. (Scale bar: 100 µm.) 4',6-diamidino-2-phnylindole (**DAPI**) stains nuclei blue. *(C)* a-CTNNB1 protein expression (red) evaluated in the presence of the WNT activator, CHIR99021. DAPI nuclei labeling is shown in blue. Merged fluorescence images overlay a-CTNNB1 and DAPI images. (Scale bar: 500 µm.) *(D)* Phase contrast images depicting cell morphology of EVT cells in control conditions or in the presence of CHIR99021 on day 8 of EVT cell

differentiation. (Scale bar: 500 μm.) *(E)* Transcript levels for EVT cell associated transcripts: HLA-G, MMP2 and ASCL2 on day 8 of EVT cell differentiation in control conditions or in the presence of CHIR99021, n=3, Graphs represent mean values ± standard error of the mean (**SEM**), one-way ANOVA, Tukey's post hoc test, ****P<0.0001. *(F)* HLA-G (green) expression was assessed by immunofluorescence following exposure to CHIR99021 for 8 days under conditions to promote EVT cell differentiation. DAPI positive nuclei labeling is shown in blue. Merged fluorescence images overlay HLA-G and DAPI images. (Scale bar: 500 μm.) *(G and H)* A volcano plot and a heat map depicting RNA-seq analysis of control and CHIR99021 treated EVT cells (n=3 per group). *(G)* Blue dots represent significantly down-regulated transcripts (P≤0.05) and a logarithm of base two-fold change of less than or equal to −2. Red dots represent significantly up-regulated transcripts with P≤0.05 and a logarithm of base two-fold change of ≥2. *(H)* Heat map colors represents z-scores of reads per kilobase per million (**RPKM**) values. *(I)* Matrigel invasion assay of control or CHIR9902 treated cells under conditions promoting EVT cell differentiation. *(J)* The relative number of invading cells of control and CHIR9902 treated cells. Mean values ± SEM are presented, n=3, unpaired t-test, ****P<0.0001.

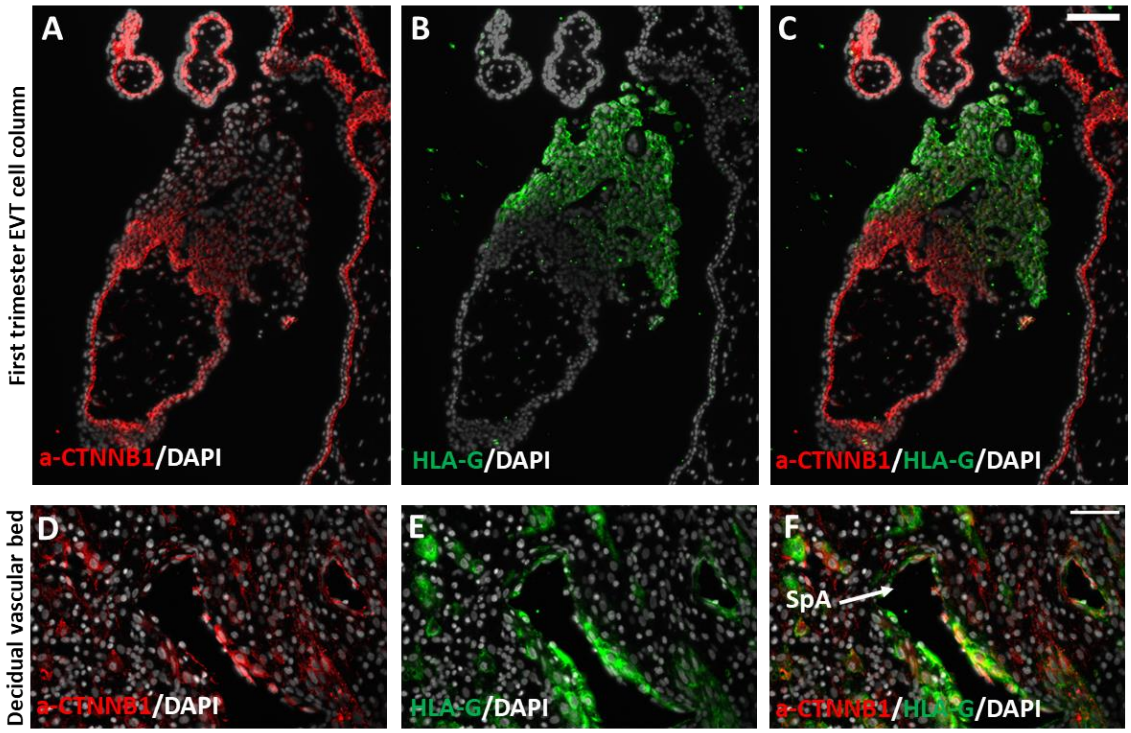

Fig. 2. Immunofluorescence of first trimester human placenta at 12 weeks of gestation tested for the presence of active CTNNB1 (**a-CTNNB1**; red) and HLA-G (green)**.** *(A)* a-CTNNB1 is expressed in cytotrophoblast, whereas *(B)* HLA-G (red) is expressed in EVT column cells but not in cytotrophoblast or syncytiotrophoblast compartments**.** *(C)* Merged fluorescence images overlay a-CTNNB1 (red) and HLA-G (green). First trimester human uteroplacental tissue immunostained for *(D)* a-CTNNB1 (red) and *(E)* HLA-G (green). *(F)* Merged fluorescence images overlay a-CTNNB1 (red) and HLA-G (green). The arrow indicates endovascular EVT cells lining a decidual spiral arteriole (SpA). DAPI positive nuclei labeling is shown in grey. Scale bar: 50 µm.

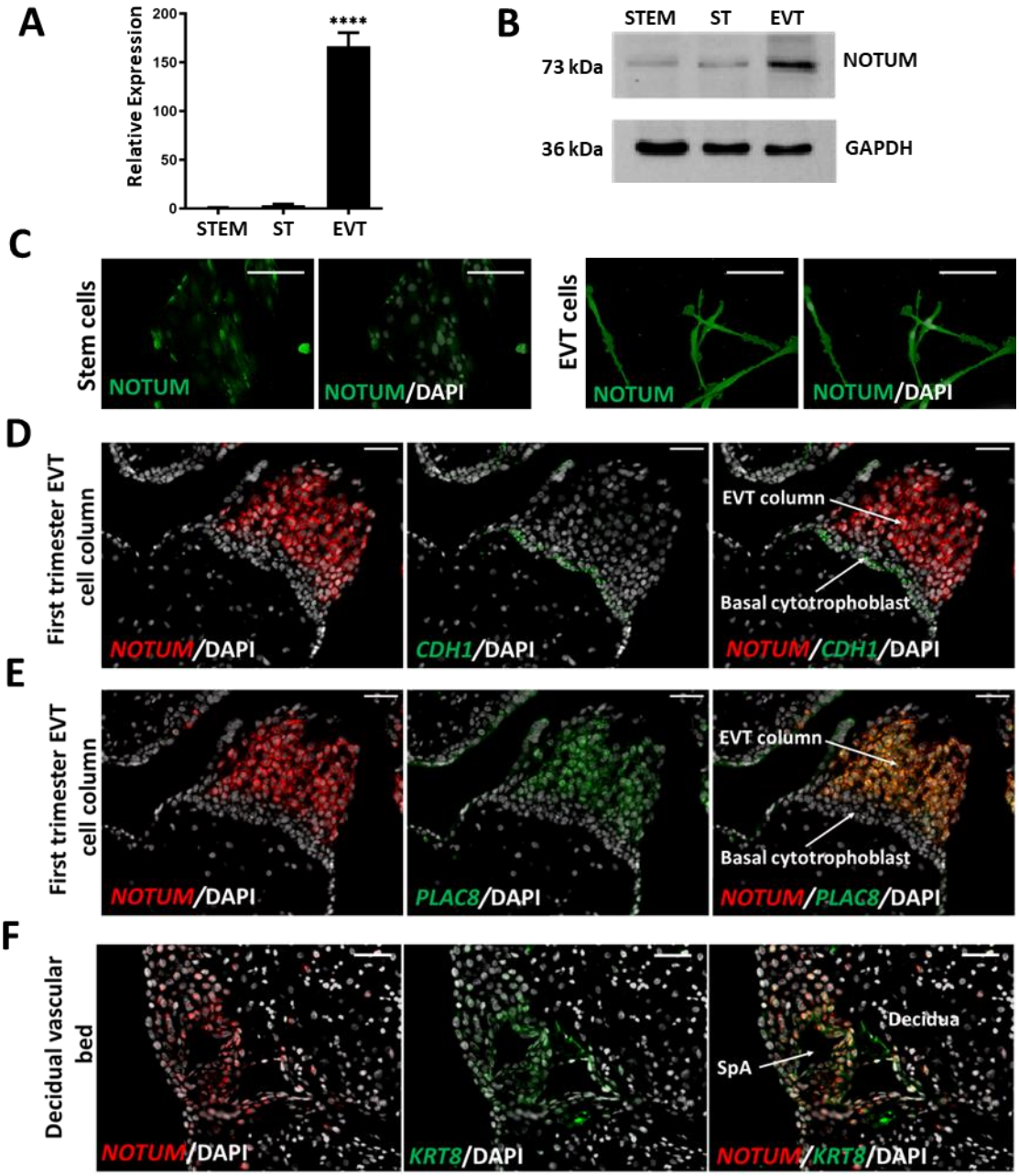

Fig. 3. NOTUM is expressed in EVT cells. *(A)* Transcript levels of *NOTUM* in TS cells maintained in the stem state (**STEM**) or induced to differentiate into syncytiotrophoblast (ST) or EVT cells. Graphs represent mean values ± SEM, one-way ANOVA, Tukey's post hoc test, n=4, ****P<0.0001. *(B)* Western blot detection of NOTUM and GAPDH expression in TS cells maintained in the stem state (**STEM**) or induced to differentiate into ST or EVT cells. *(C)* Immunofluorescence localization of NOTUM protein in TS cells maintained in the stem state or induced to differentiate into EVT cells. DAPI positive nuclei labeling is shown in grey. *(D, E)* In situ hybridization of first trimester human placenta at 12 weeks of gestation probed for *NOTUM* (red), *CDH1* (green), or *PLAC8* (green). *NOTUM* (red) is expressed in EVT cell columns but not in basal cytotrophoblast. DAPI positive nuclei labeling is shown in grey. Scale bars: 50 µm. *(F)* In situ hybridization of decidual vascular bed tissue probed for *NOTUM* (red) and *KRT8* (green) using in situ hybridization. DAPI positive nuclei labeling is shown in grey. The arrow indicates endovascular EVT cells lining a decidual spiral arteriole (**SpA**). Merged fluorescence images of *NOTUM*, *KRT8*, and DAPI. Scale bars: 50 µm

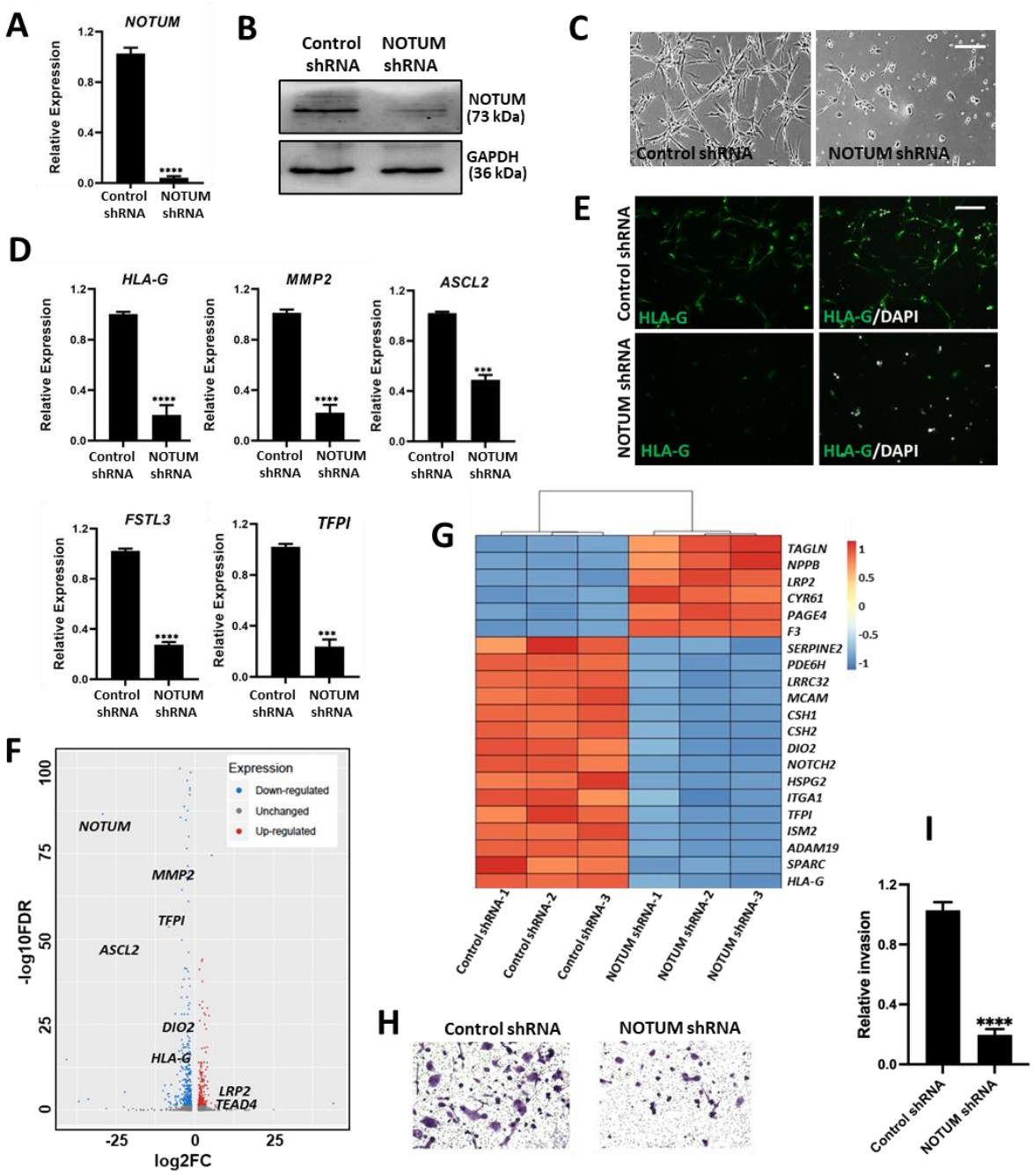

Fig. 4. NOTUM regulates EVT cell differentiation. Effectiveness of NOTUM shRNA treatment was determined by *(A)* RT-qPCR and *(B)* western blotting. GAPDH was used as a loading control for the western blot. *(C)* Phase contrast images depicting cell morphology of TS cells cultured in conditions to promote EVT cell differentiation transduced with control shRNA or NOTUM shRNA. Scale bar: 200 µm. *(D)* Transcript levels of EVT cell markers (*HLA-G*, *MMP2*, *ASCL2*, *FSTL3*, and *TFPI*) in control shRNA and NOTUM shRNA treated cells following exposure to conditions that promote EVT cell differentiation. NOTUM knockdown decreased levels of transcripts characteristic of EVT cells (n=3 transductions), Graphs represent mean values ± SEM, n=3, unpaired t-test ****P<0.0001. *(E)* Immunofluorescence of HLA-G (green) in control shRNA and NOTUM shRNA treated cells following exposure to conditions that promote EVT cell differentiation. DAPI positive nuclei are shown in blue. Merged fluorescence images of HLA-G and DAPI. Scale bar: 500 µm. *(F and G)* A volcano plot and a heat map depicting RNA-seq analysis of control shRNA and NOTUM shRNA treated EVT cells (n=3 per group). *(F)* Blue dots represent significantly down-regulated transcripts (P≤0.05) and a logarithm

of base two-fold change of less than or equal to −2. Red dots represent significantly up-regulated transcripts with P≤0.05 and a logarithm of base two-fold change of ≥2. *(G)* Heat map of control control shRNA and NOTUM shRNA treated TS cells induced to differentiate into EVT cells. Colors represents z-scores of RPKM values. *(H)* Matrigel invasion assay of control shRNA or NOTUM shRNA treated cells under conditions promoting EVT cell differentiation. *(I)* The relative number of invading cells of control shRNA and NOTUM shRNA treated cells, Graphs represent mean values ± SEM, n=3, unpaired t-test, ****P<0.0001.

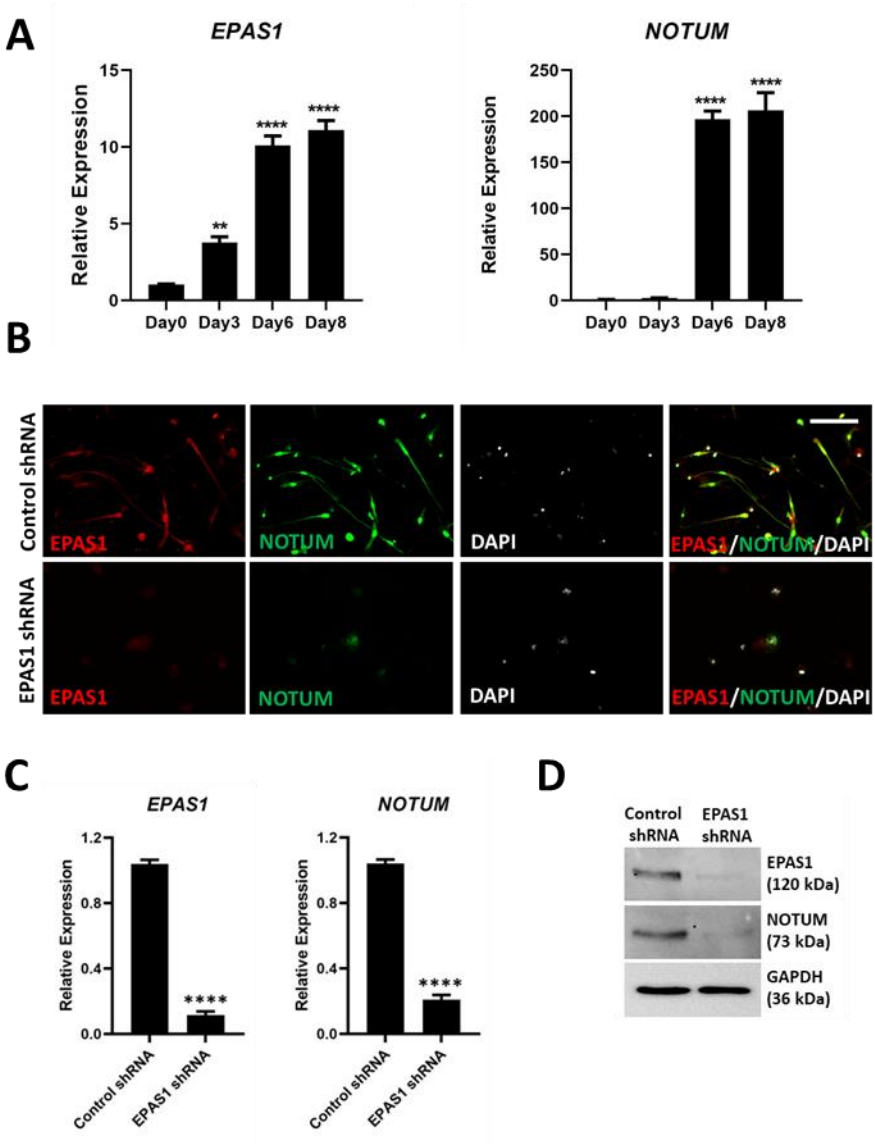

Fig. 5. Upstream regulation of NOTUM in EVT cells. (*A*) Time course of *EPAS1* and *NOTUM* from stem state (Day 0) and days 3, 6, and 8 of EVT cell differentiation. Graphs represent mean values ± SEM, one-way ANOVA, Tukey's post hoc test, n=4, **P<0.01, ****P<0.0001 *(B)* Immunofluorescence of EPAS1/HIF2A (red) and NOTUM (green) in TS cells induced to differentiate into EVT cells following transduction with lentivirus containing control shRNA or EPAS1 shRNA. DAPI positive nuclei labeling is shown in grey. Merged fluorescence images EPAS1, NOTUM and DAPI. Scale bar: 500 µm. Effects of EPAS1 shRNA knockdown on EPAS1 and NOTUM expression assessed by (*C*) RT-qPCR, graphs represent mean values ± SEM, n=3, unpaired *t*-test ****P<0.0001 and (*D*) western blotting.

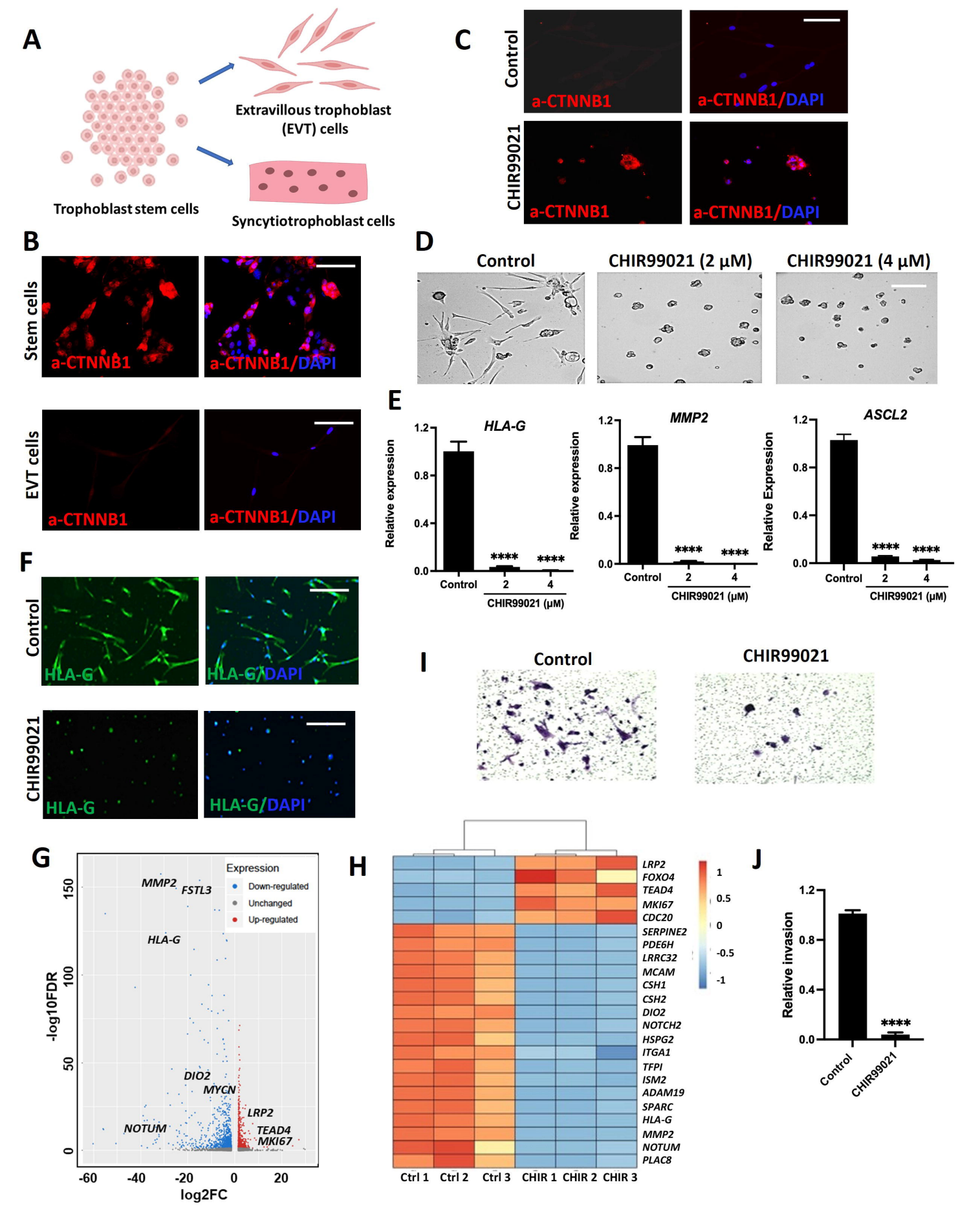
A
Extravillous trophoblast (EVT) cells
Trophoblast stem cells
Syncytiotrophoblast cells
B
Stem cells
EVT cells
a-CTNNB1
a-CTNNB1/DAPI
C
Control
CHIR99021
a-CTNNB1
a-CTNNB1/DAPI
D
Control
CHIR99021 (2 μM)
CHIR99021 (4 μM)
E
HLA-G
MMP2
ASCL2
Relative expression
Relative Expression
Control
2
4
CHIR99021 (μM)
****
F
Control
CHIR99021
HLA-G
HLA-G/DAPI
I
Control
CHIR99021
G
Expression
Down-regulated
Unchanged
Up-regulated
MMP2
FSTL3
HLA-G
DIO2
MYCN
LRP2
NOTUM
TEAD4
MKI67
-log10FDR
log2FC
H
LRP2
FOXO4
TEAD4
MKI67
CDC20
SERPINE2
PDE6H
LRRC32
MCAM
CSH1
CSH2
DIO2
NOTCH2
HSPG2
ITGA1
TFPI
ISM2
ADAM19
SPARC
HLA-G
MMP2
NOTUM
PLAC8
Ctrl 1
Ctrl 2
Ctrl 3
CHIR 1
CHIR 2
CHIR 3
J
Relative invasion
Control
CHIR99021

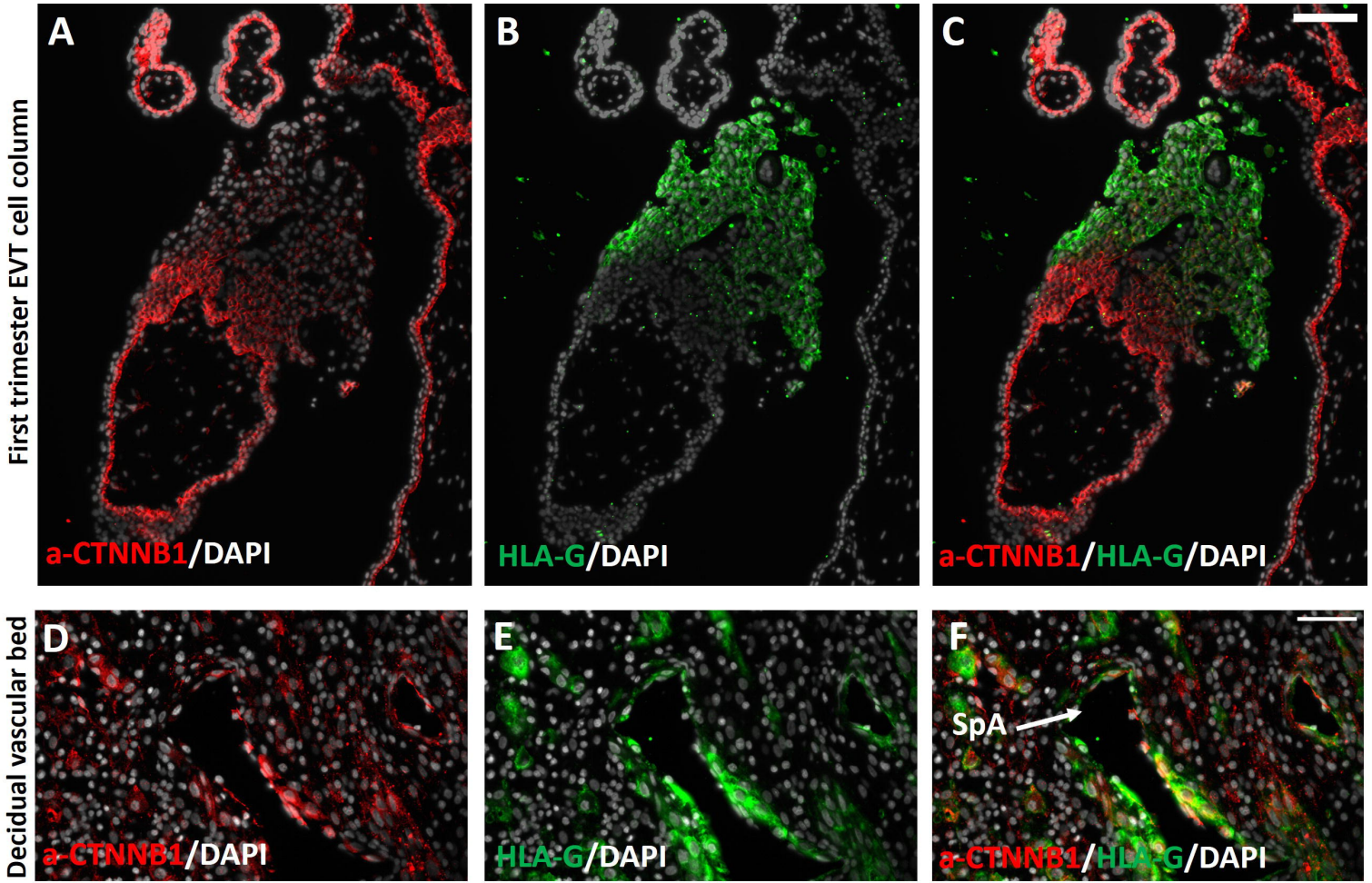
First trimester EVT cell column
A
a-CTNNB1/DAPI
B
HLA-G/DAPI
C
a-CTNNB1/HLA-G/DAPI
Decidual vascular bed
D
a-CTNNB1/DAPI
E
HLA-G/DAPI
F
SpA
a-CTNNB1/HLA-G/DAPI

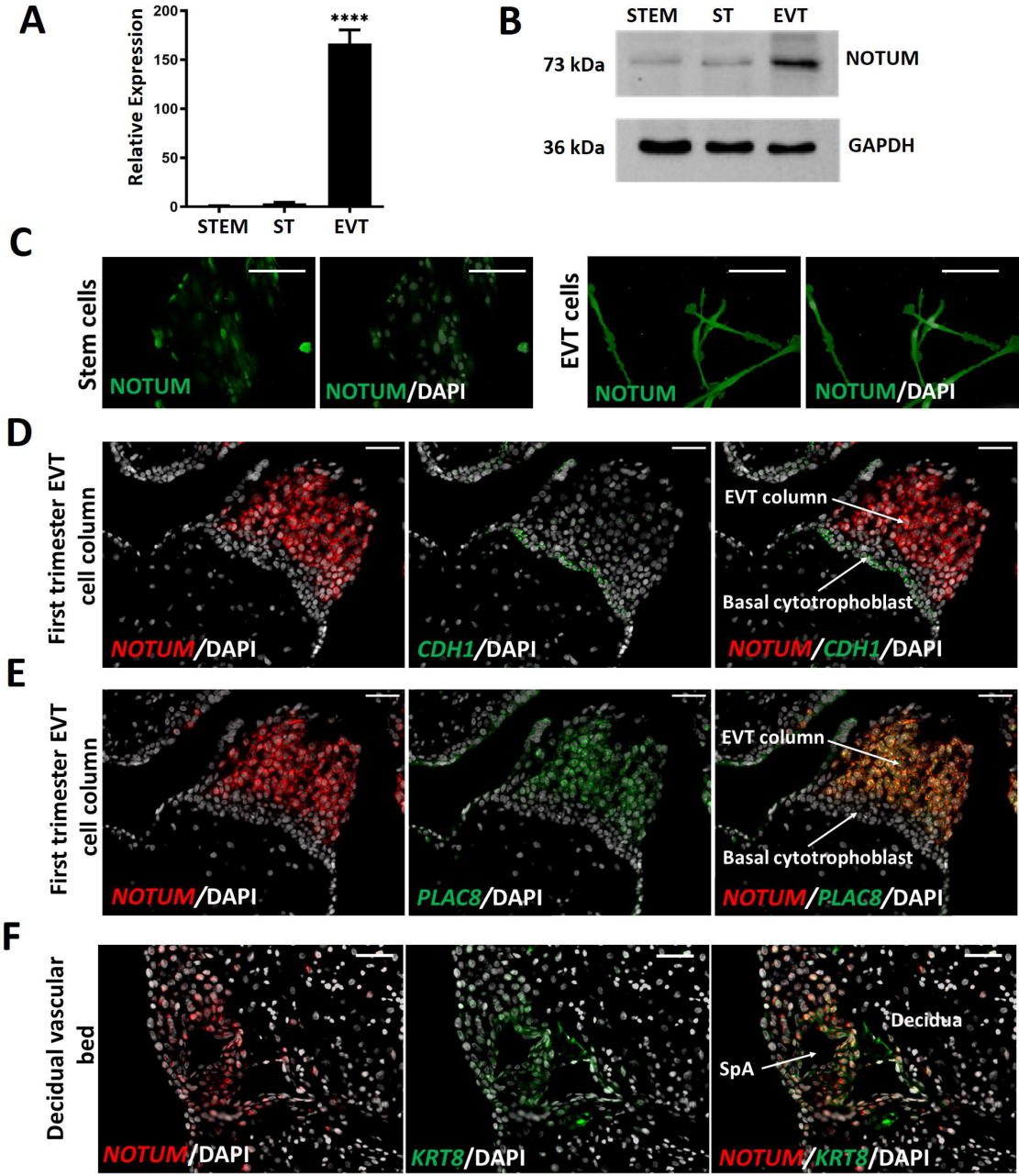
A
Relative Expression
200
150
100
50
0
****
STEM
ST
EVT
B
STEM
ST
EVT
73 kDa
NOTUM
36 kDa
GAPDH
C
Stem cells
NOTUM
NOTUM/DAPI
EVT cells
NOTUM
NOTUM/DAPI
D
First trimester EVT cell column
NOTUM/DAPI
CDH1/DAPI
EVT column
Basal cytotrophoblast
NOTUM/CDH1/DAPI
E
First trimester EVT cell column
NOTUM/DAPI
PLAC8/DAPI
EVT column
Basal cytotrophoblast
NOTUM/PLAC8/DAPI
F
Decidual vascular bed
NOTUM/DAPI
KRT8/DAPI
Decidua
SpA
NOTUM/KRT8/DAPI

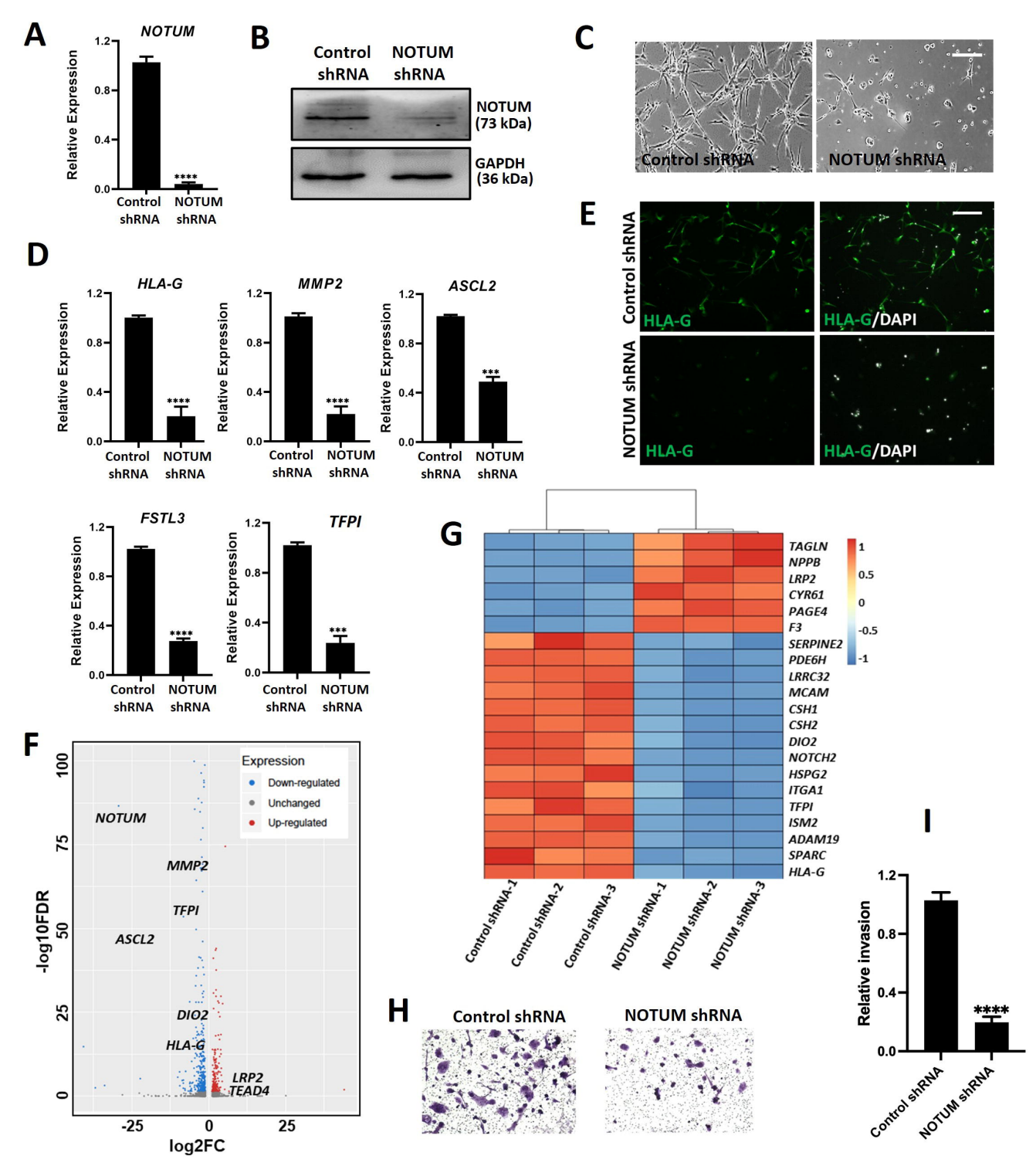
A
NOTUM
Relative Expression
1.2
0.8
0.4
0.0
****
Control shRNA
NOTUM shRNA
B
Control shRNA
NOTUM shRNA
NOTUM (73 kDa)
GAPDH (36 kDa)
C
Control shRNA
NOTUM shRNA
D
HLA-G
MMP2
ASCL2
FSTL3
TFPI
Relative Expression
****
***
Control shRNA
NOTUM shRNA
E
Control shRNA
NOTUM shRNA
HLA-G
HLA-G/DAPI
F
Expression
Down-regulated
Unchanged
Up-regulated
NOTUM
MMP2
TFPI
ASCL2
DIO2
HLA-G
LRP2
TEAD4
-log10FDR
log2FC
G
TAGLN
NPPB
LRP2
CYR61
PAGE4
F3
SERPINE2
PDE6H
LRRC32
MCAM
CSH1
CSH2
DIO2
NOTCH2
HSPG2
ITGA1
TFPI
ISM2
ADAM19
SPARC
HLA-G
Control shRNA-1
Control shRNA-2
Control shRNA-3
NOTUM shRNA-1
NOTUM shRNA-2
NOTUM shRNA-3
H
Control shRNA
NOTUM shRNA
I
Relative invasion
****
Control shRNA
NOTUM shRNA

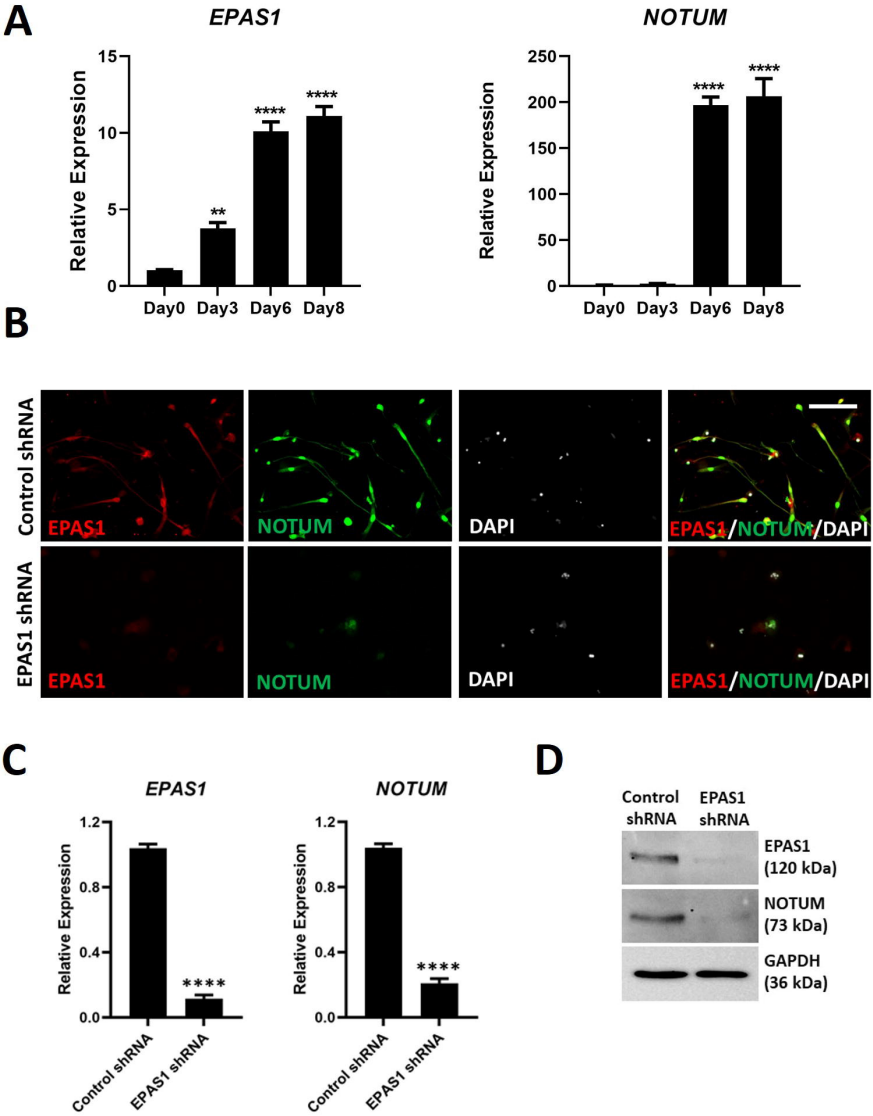
A
EPAS1
Relative Expression
15
10
5
0
**
****
****
Day0
Day3
Day6
Day8
NOTUM
Relative Expression
250
200
150
100
50
0
****
****
Day0
Day3
Day6
Day8
B
Control shRNA
EPAS1 shRNA
EPAS1
NOTUM
DAPI
EPAS1/NOTUM/DAPI
C
EPAS1
Relative Expression
1.2
0.8
0.4
0.0
****
Control shRNA
EPAS1 shRNA
NOTUM
Relative Expression
1.2
0.8
0.4
0.0
****
Control shRNA
EPAS1 shRNA
D
Control shRNA
EPAS1 shRNA
EPAS1 (120 kDa)
NOTUM (73 kDa)
GAPDH (36 kDa)